ACS Sustainable Chemistry & Engineering

Research Article

pubs.acs.org/journal/ascecg

Synthesis and Characterization of AN-*g*-SOY for Sustainable Polymer Composites

Vijay Kumar Thakur and Michael R. Kessler*

School of Mechanical and Materials Engineering, Washington State University, Pullman, Washington 99164-2920, United States

ABSTRACT: Biobased materials are rapidly emerging as alternatives to petroleum-based materials because of rising environmental awareness and augmented consumption of nondegradable polymers. In the present work, the surface characteristics of biorenewable soy flour (SOY) were tailored via free radical-induced graft copolymerization of acrylonitrile (AN) to develop novel materials for multifunctional applications. A number of reaction parameters were optimized to maximize the level of grafting. The synthesized acrylonitrile-grafted soy (AN-*g*-SOY) copolymers were characterized using Fourier transform infrared spectroscopy (FTIR), scanning electron microscopy (SEM), and thermogravimetric analysis (TGA). Polymer composites were prepared using SOY/AN-*g*-SOY as reinforcement and poly(methyl methacrylate) (PMMA) as the matrix. Dynamic mechanical analysis results showed that acrylonitrile-grafted SOY exhibited significantly enhanced storage modulus compared to polymer composites reinforced with pristine soy flour.

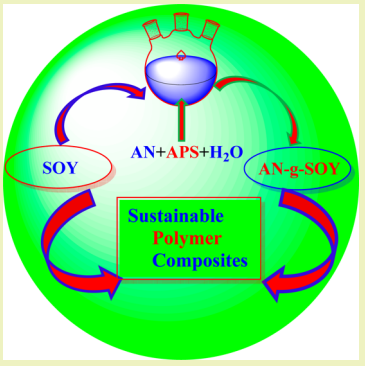

KEYWORDS: *Sustainable materials, Soy, Graft copolymerization, Composites, Dynamic mechanical analysis*

INTRODUCTION

The last few decades have seen an enormous interest in the use of polymer-based materials for a number of applications ranging from biomedical to automotive as well as components of aircraft due to their outstanding properties such as low cost, great versatility, low density, copious availability, ease of processing, little damage during processing, tailoring ability, etc.[1−4] In particular, the lightweight characteristics of polymer-based materials have a direct impact on the fuel economy in the automotive field.[5−8] Biorenewable polymers in particular are rapidly emerging as alternatives to traditional synthetic polymers due to the nonbiodegradable nature of the synthetic polymers combined with environmental and health risks.[9−12] Some biorenewable polymeric materials derived from different natural resources offer a number of significant advantages over petroleum-based polymeric materials, including biodegradability, environmental friendliness, acceptable specific strength and modulus, low cost, acoustic properties, nonabrasive surfaces, low density, ready availability, and easy recyclability.[13−16] Different kinds of biorenewable polymers have been used, in particular in the preparation of polymer composites.[16,17] In fact, biobased polymer composites have replaced synthetic fiber-based polymer composites in a number of applications.[18−21]

Soy-based materials, such as soy protein, soy concentrate, and soy flour, offer biodegradability, renewability, economically competitive cost, functional properties, and environmental friendliness, among other properties.[22−24] For these inherent properties, soy-based materials have been explored recently as components in novel polymer composites[25−27] that exhibit enhanced energy recovery, lower greenhouse gas emissions, low dependence on nonrenewable energy, no dependence on petrochemical resources, and lower pollutant emissions.[13,28] However, the use of soy as a reinforcement in polymer composites has been restricted because of its high water and moisture absorption and low thermal stability during processing, as well as poor adhesion with the hydrophobic polymers used as matrix materials.[16] Water/moisture absorption in the polymer composites ultimately leads to the degradation of the composites.[9] Typically, this degradation starts at the fiber−matrix interface region and leads to poor stress transfer efficiencies and a reduction in mechanical and other properties.[9]

Several studies reported that suitable surface modification techniques can efficiently reduce the moisture sensitivity of certain physicochemical, mechanical, and thermal properties of the polymers.[9,29] A variety of techniques have been used to alter the surface characteristics of biobased polymers,[11,30−32] among which graft copolymerization was a promising method to design biorenewable polymers with specific functionalities. Graft copolymerization is a highly effective way to incorporate hydrophobic characteristics in a numbers of polymers. It also improves the compatibility between the matrix materials and the reinforcement.[33]

The existing literature provides limited information on the use of vinyl monomers for graft copolymerization of soy flour to incorporate hydrophobic characteristics. The present paper tries to explore the potential utilization of an acrylonitrile monomer to graft copolymerize soy. The present work will study the synthesis and characterization of acrylonitrile-grafted

Received: July 22, 2014
Revised: August 26, 2014
Published: September 3, 2014

soy (AN-*g*-SOY) and the utilization of AN-*g*-SOY in the preparation of polymer composites.

EXPERIMENTAL SECTION

Materials. Soy flour (SOY) was procured from ADM Specialty Products-Oilseeds, Decatur, IL, U.S.A. The reaction monomer acrylonitrile (AN) used, the initiator, ammonium persulfate (APS), and poly(methyl methacrylate) (PMMA were purchased from Sigma-Aldrich. All chemicals were used as received, without additional purification.

Synthesis of Acrylonitrile-Grafted SOY Copolymers (AN-*g*-SOY). A solution with a pH between 10 and 12 was prepared in a reaction flask by the slow addition of sodium hydroxide prior to initializing graft copolymerization. To this solution, 2 g of SOY was added and stirred well for 60 min at 95 °C to form a homogeneous suspension. Sodium metabisulfite was then slowly added to this homogeneous solution to cleave the disulfide bonds and facilitate graft copolymer synthesis. The reaction was carried out at 85 °C for 2 h to ensure the efficient cleavage of the disulfide bonds. The reaction temperature was then lowered to 75 °C, followed by the addition of specific amounts of the APS initiator and AN monomer. The resulting solution was allowed to react at 60 °C, and after 5 h, the reaction was ended. The material formed by graft copolymerization was poured into an excess solution of sodium hydroxide to precipitate the graft AN-*g*-SOY copolymers. The graft copolymer sample was thoroughly washed with distilled water and then dried. In order to further remove any traces of polyacrylonitrile homopolymer (formed during grafting/self-polymerization), the AN-*g*-SOY copolymer was Soxhlet extracted with dimethylformamide (DMF) at ambient laboratory conditions for 24 h. The extracted AN-*g*-SOY samples were then dried at 50 °C for 24 h. The percentage of grafting was calculated using the following equation[25]

$$(P_g) = \frac{W_g - W}{W} \times 100$$

where W is the weight of pristine SOY, and W_g is the weight of AN-*g*-SOY

Preparation of Polymer Composite Films. Pristine SOY and AN-*g*-SOY samples were dried in a hot air oven at 70 °C for 24 h to remove any moisture content. Subsequently, PMMA and SOY/AN-*g*-SOY with an AN-*g*-SOY loading of 5 wt % were melt processed at 200 °C using a twin screw microcompounder. In order to ensure melt homogenization, the residence time of the (SOY/AN-*g*-SOY)/PMMA melt in the barrel was maintained at 5 min. The extruded samples were pelletized and compression molded at 210 °C to prepare 50 mm × 50 mm × 1 mm films using a compression molding machine.

Characterization of Pure SOY and AN-*g*- SOY Copolymer Films. Infrared spectra of pure SOY and AN-*g*-SOY were obtained using Fourier transform infrared spectroscopy (FTIR). Thermogravimetric analyses for all samples were performed using a TGA-Q50 from TA Instruments (New Castle, DE, U.S.A.) in a nitrogen atmosphere at a heating rate of 20 °C/min. Samples weighing approximately 10 mg were used in each experiment. The surface morphology of the samples was examined by scanning electron microscopy (SEM, SUPRA35, Zeiss, Germany). Dynamic mechanical analyses for different samples were performed in a dynamic mechanical analyzer (DMA model Q800) from TA Instruments (New Castle, DE, U.S.A.). The experiments were performed in tensile mode. Temperature sweep tests were conducted at temperatures between −100 and 140 °C at a frequency of 1 Hz, with a strain amplitude of 0.05% and at a heating rate of 3 °C/min.

RESULTS AND DISCUSSION

Biorenewable-based polymeric materials are considered materials of the future because of their inherent properties, in particular environmental friendliness and low cost. Biobased materials, for example, soy flour (SOY), soy protein concentrate (SPC), and soy protein isolate (SPI) are low-cost materials and have been used in the preparation of green polymer composites.[23−28] Among the different derivatives of soybean, soy in the form of soy protein concentrate (SPC) and soy protein isolate (SPI) has been frequently used as matrix materials in green composites. However, limited attention has been paid to the use of soy flour in the preparation of polymer composites in spite of the fact that it is the cheapest derivative of soybean and is frequently considered a waste material.[24] Soy flour is mainly composed of protein and carbohydrates (approximately 56%). The availability of hydroxyl and amino groups on the soy backbone facilitates the modification of soy flour through free radical-induced graft copolymerization.[25] In the present work, the initiator (APS) played an important role during graft copolymerization of acrylonitrile (AN) onto SOY. The APS initiator facilitated the creation of reactive sites on the polymer backbone for graft copolymerization synthesis, which proceeded through three steps: chain initiation, propagation, and termination. Schemes 1 and 2 depict the mechanism of free

Scheme 1. Structural Representation of SOY.[25]

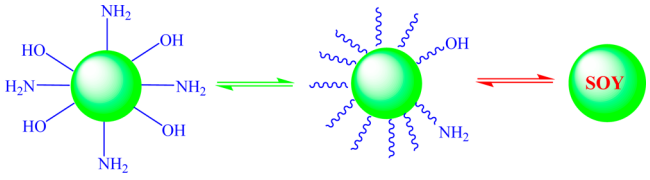

radical-induced graft copolymerization of AN onto SOY.[11,20] As is evident from Scheme 2, the synthesis of the graft copolymerization reaction starts with the formation of the free radicals (eqs 1 and 2), which are used during the three reaction steps, namely, chain initiation, propagation, and termination, as mentioned above. In the chain initiation step, the initiator radicals attacks the functional groups on SOY as well as the acrylonitrile and initiates graft copolymerization of the acrylonitrile reaction monomer onto the SOY backbone by creating the free radical sites on these two important reaction species (eqs 3−6). Subsequently, in the chain propagation step, the addition of the acrylonitrile reaction monomer to the initiated reaction further propagates graft copolymerization synthesis. It results in growing of the active graft copolymer chains (eqs 7−10). In the chain termination step, which is the last step in graft copolymerization synthesis, there is formation of the desired AN-*g*-SOY copolymers as a result of the reaction between the growing AN chains and the active SOY backbone (eqs 11−14).

To obtain a SOY copolymer with an optimum amount of grafted AN, different reaction parameters were optimized by investigating the reaction conditions, as discussed in the following section.

The amount of solvent during graft copolymerization synthesis significantly affected the degree of grafting.[11,20] Figure 1(a) shows the effect of the solvent reaction medium on the graft copolymerization of AN onto the SOY backbone. The solvent facilitated the accessibility of the AN monomer onto the SOY backbone. The figure shows that the degree of grafting increased with increasing water content until it reached a critical value, after which it decreased. This decrease was attributed to a possible inhibition of the interaction between the AN monomer and SOY and growing graft chains.

Figure 1(b) depicts the effect of reaction time on the graft copolymerization of AN onto the SOY backbone. The degree

dx.doi.org/10.1021/sc500473a | ACS Sustainable Chem. Eng. 2014, 2, 2454−2460

Scheme 2. Plausible Mechanism for Graft Copolymerization of Acrylonitrile onto SOY

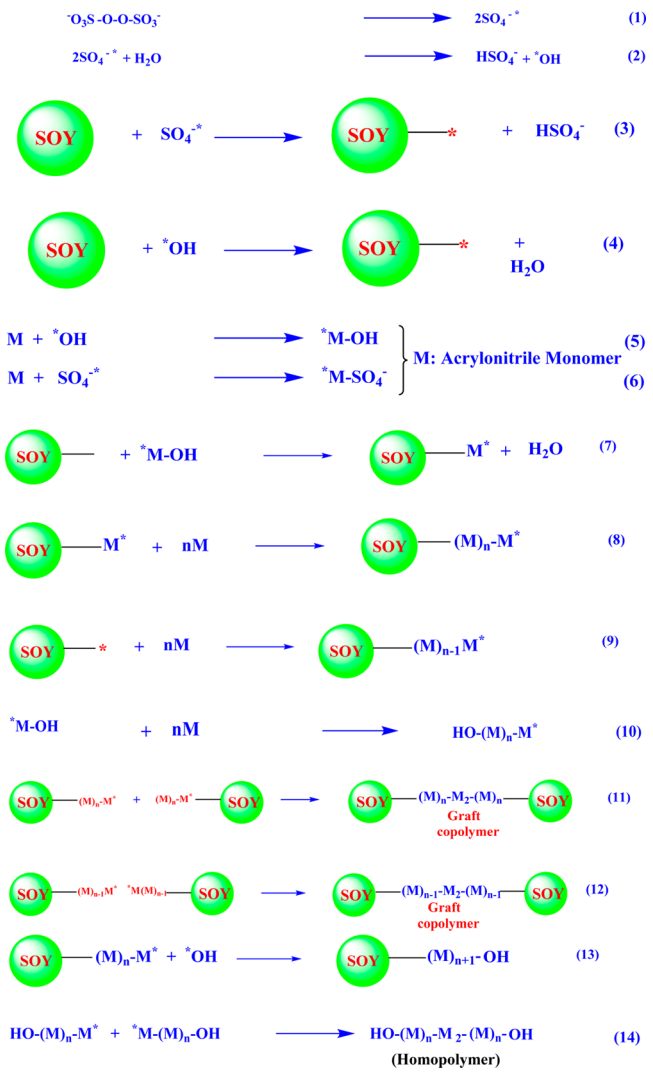

of grafting increased with increasing reaction time, and after a specific time, it slightly decreased with a further increase in reaction time.[11,20] The decrease in the degree of grafting beyond the optimum time value can be attributed to the mutual destruction of growing polymeric chains in the AN-*g*-SOY copolymers, which leads to homopolymerization of the acrylonitrile monomer radicals and backbiting by the active radicals. These results are in conformity with previous results on the graft copolymerization of vinyl monomers onto biopolymers.[11,20,29−33]

The effect of reaction temperature on the graft copolymerization of AN onto SOY was investigated over a temperature range from 20 to 70 °C, and the results are presented in Figure 1(c). The degree of grafting increased up to a temperature of 60 °C, then decreased with a further increase in temperature. The decrease in the degree of grafting beyond 60 °C was attributed to an increase in homopolymerization reactions.[11,20]

Figure 1(d) shows the effect of the amount of APS initiator on the graft copolymerization reaction. The initiator generates the free radical sites on the SOY backbone as well as in the reaction monomer. With an increase in initiator amount, a large number of macroradicals are formed as a result of the interaction between the free radicals and the functional groups of the SOY (Scheme2). However, this increase was observed only until an optimum concentration of initiator was reached. Beyond this concentration, the degree of grafting decreased. With excess levels of initiator, the free radicals mainly reacted with the AN monomer instead of SOY and thus led to homopolymerization of the monomer.[11,20]

Figure 1(e) shows the effect of monomer (AN) concentration on the level of grafting, which initially increased with an increase in concentration because of the abundant availability of the AN monomer in the proximity of the SOY macroradicals. However, at monomer concentrations higher than approximately 0.9 mL/L, the degree of grafting decreased because most of the reactive sites on SOY were already reacted at the optimum monomer concentration. There were no sites available for further reaction of AN with SOY, causing AN homopolymerization and leading to a decrease in the degree of grafting.[11,20]

Characterization of Pristine SOY and AN-*g*-SOY Copolymer. The FTIR spectra of pristine SOY and AN-*g*-SOY are shown in Figure 2. In the spectra of pristine SOY, the characteristic bands at 3407, 1667, and 1547 cm^{-1} can be assigned to the stretching mode of the O−H/N−H groups, C═O stretching of the amide group (amide-I), and N−H bending (amide−II), respectively. The spectra of AN-*g*-SOY exhibited several new characteristic bands reflecting the presence of AN. The peak of AN-*g*-SOY at 2243 cm^{-1} was attributed to the nitrile groups (−C≡N) and confirmed the successful grafting of acrylonitrile onto SOY.

Thermogravimetric analysis (TGA) of pristine SOY and AN-*g*-SOY was performed as a function of percentage weight loss versus temperature in a nitrogen atmosphere. Figure 3 shows that pristine SOY decomposed in three stages as a result of the thermal degradation of its different constituents. The first stage of decomposition between 40 and 210 °C was attributed to the dissociation of the structure of SOY (proteins and carbohydrates) along with the elimination of moisture content/water molecules. The second decomposition phase occurred between 210 and 500 °C as a result of the cleavage of different peptide bonds/structural bonds of the protein/carbohydrate moieties. The third phase of decomposition (between 500 and 880 °C) was attributed to the complete degradation of the proteins and carbohydrates present in SOY. AN-*g*-SOY thermal decomposition occurred in two phases (Figure 4). The first phase was between 230 and 470 °C, and the second phase was between 470 to 890 °C. A comparison of the two thermograms showed that the thermal stability of SOY improved to a significant extent as a result of graft copolymerization. The increase in thermal stability was attributed to the covalent bonding of AN onto SOY as shown in Scheme 2. Due to graft copolymerization, the hydrophilic groups on SOY are replaced by hydrophobic polyacrylonitrile groups that enhance the thermal stability of the SOY due to its inherent higher thermal stability compared to the pristine SOY. These results were further supported by the corresponding DTG results of pristine SOY and AN-*g*-SOY.

The scanning electron micrographs of the pristine SOY and AN-*g*-SOY in Figures 5 and 6 depict the significant transformation of the surface morphology of SOY under free radical-induced graft copolymerization with acrylonitrile. Pristine SOY exhibited a smooth morphology compared to AN-*g*-SOY. The changes in morphology of SOY induced by free radical graft copolymerization were attributed to the covalent bonding of

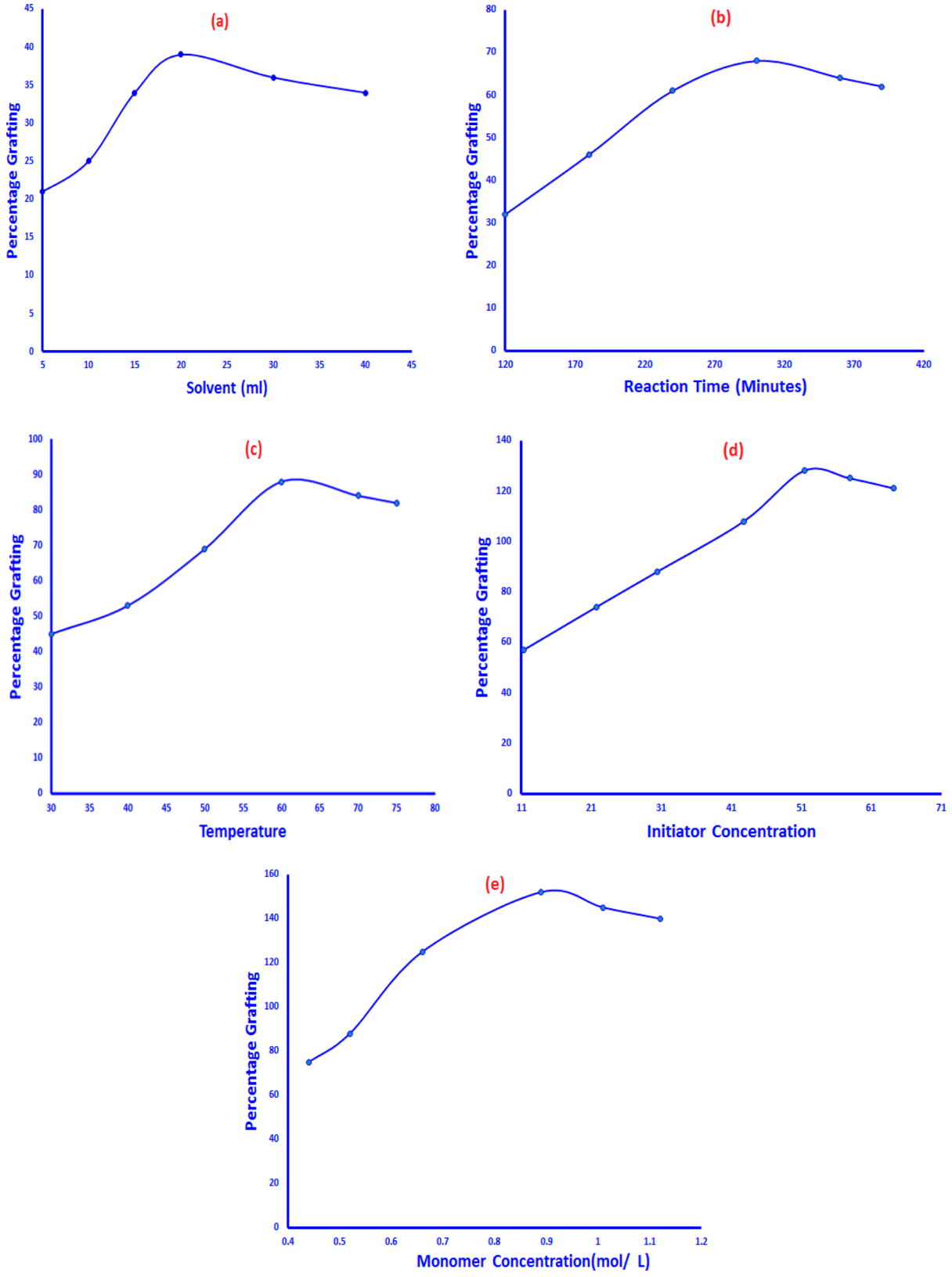

Figure 1. Percentage of grafting (a) as a function of solvent, (b) as a function of reaction time, (c) as a function of reaction temperature, (d) as a function of initiator concentration, and (e) as a function of monomer concentration.

the AN monomer with the peptide/S−S linkages and OH groups.

Preparation of SOY-Reinforced Polymer Composites. Polymer composites were prepared using PMMA as the matrix material and pristine SOY and AN-*g*-SOY as the reinforcements to study the effect of incorporation of hydrophobic functionalities into the SOY. Compared to the pristine SOY, which is hydrophilic in nature due to the presence of hydroxy

dx.doi.org/10.1021/sc500473a | *ACS Sustainable Chem. Eng.* 2014, 2, 2454−2460

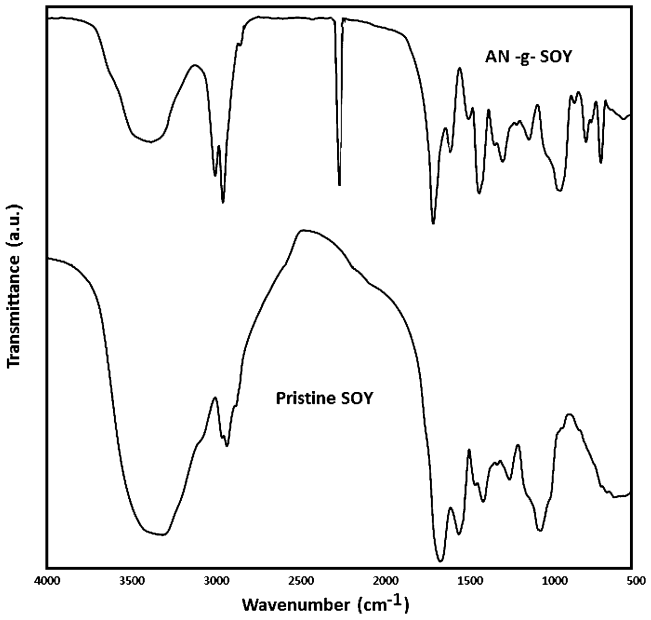

Figure 2. FTIR spectra of pristine SOY and AN-*g*-SOY.

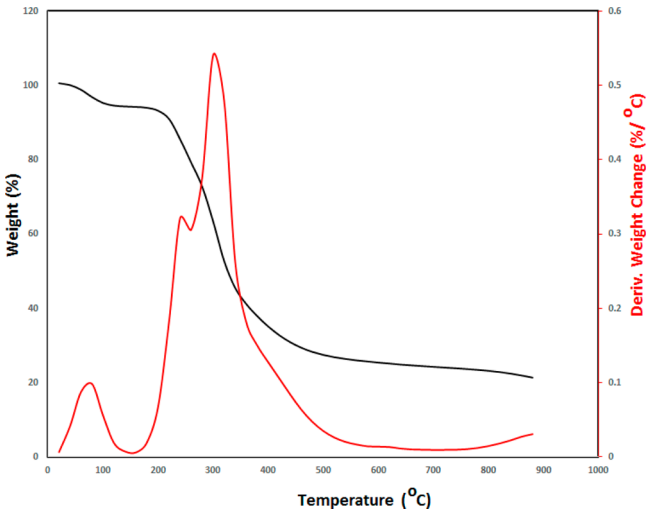

Figure 3. TGA/DTG of pristine SOY.

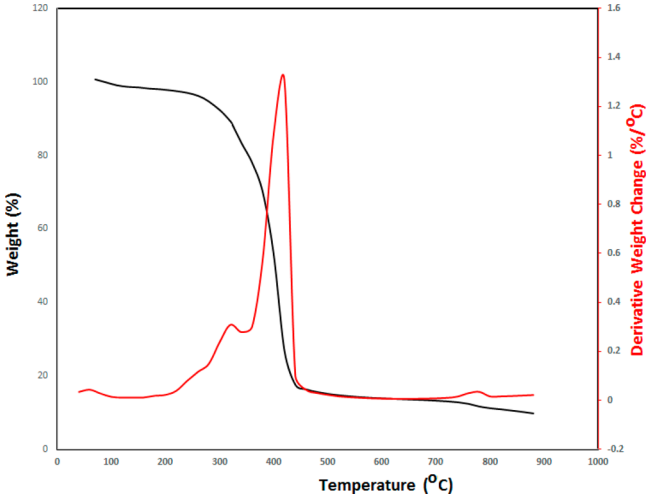

Figure 4. TGA/DTG of AN-*g*-SOY.

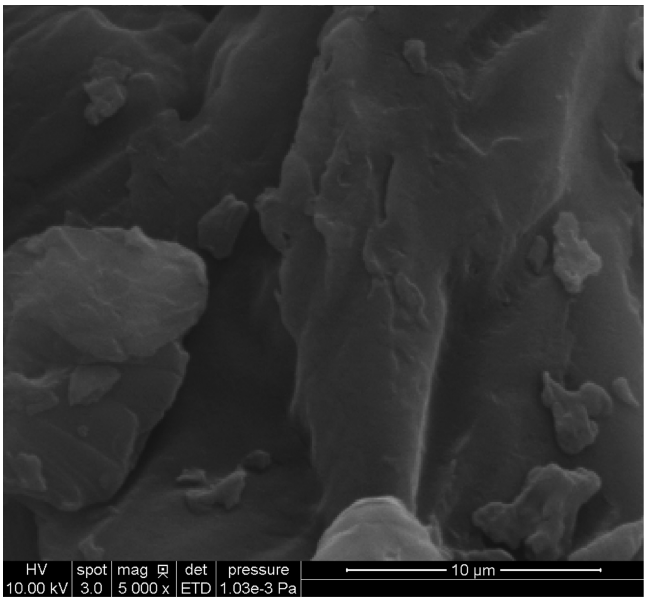

Figure 5. Scanning electron micrograph of pristine SOY.

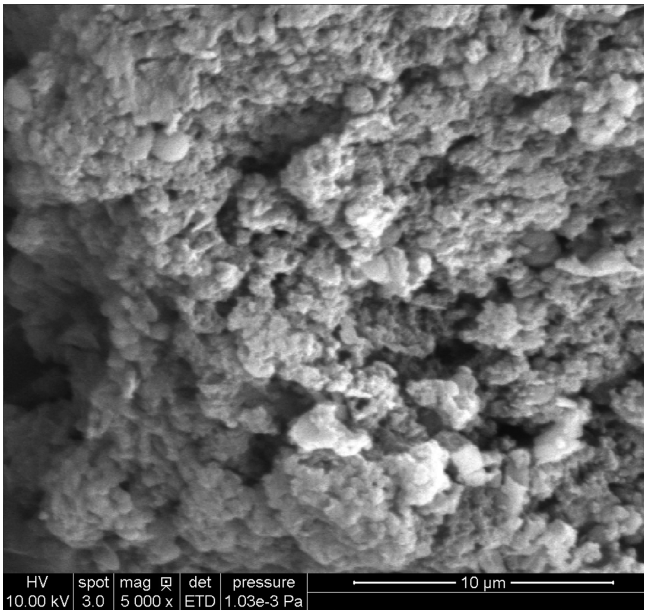

Figure 6. Scanning electron micrographs of AN-*g*-SOY.

and amino groups, the acrylonitrile grafted SOY is expected to be quite hydrophobic because of the replacement of these groups by the strong hydrophobic groups of AN. The presence of these functional groups strongly increases the resistance of the AN-*g*-SOY copolymer against moisture absorbance and other wettability studies.

Subsequently, the dynamic mechanical analysis of the (SOY/AN-*g*-SOY)/PMMA polymer composites was studied. The dynamic mechanical analysis results of the different tested samples, namely, pristine PMMA, PMMA/SOY composites, and PMMA/AN-*g*-SOY composites prepared using 5 wt % loadings are shown in Figures 7−9. These figures depict the storage modulus and damping coefficient (tan $\delta = E''/E$) of the studied samples. The storage modulus of any sample generally refers to the stiffness of a material. Figures 7−9 show the effect of temperature on the storage modulus (E') along with the

dx.doi.org/10.1021/sc500473a | *ACS Sustainable Chem. Eng.* 2014, 2, 2454−2460

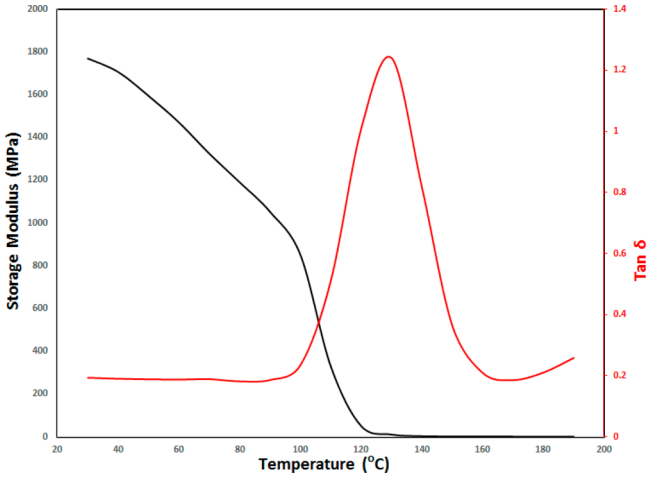

Figure 7. Storage modulus and tan δ curves of pristine PMMA determined by dynamical mechanical analysis.

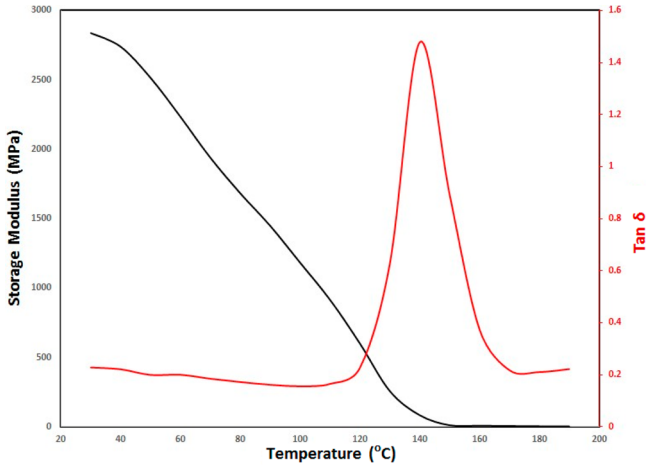

Figure 8. Storage modulus and tan δ curves of the SOY/PMMA composite determined by dynamical mechanical analysis.

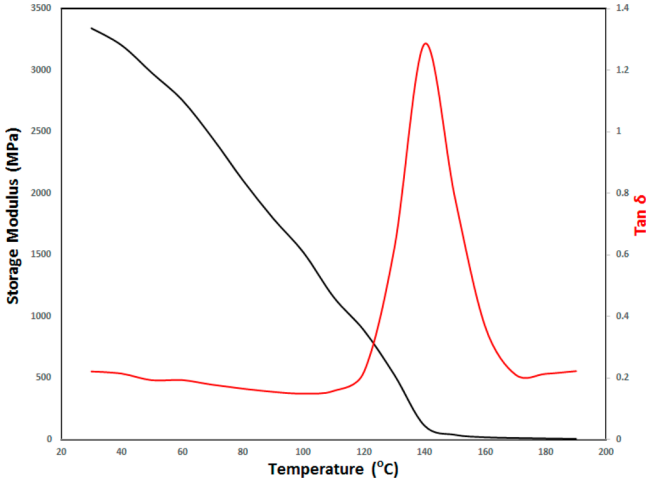

Figure 9. Storage modulus and tan δ curves of the AN-*g*-SOY/PMMA composite determined by dynamical mechanical analysis.

damping coefficient (tan $\delta = E''/E$). These studies were carried out on the rectangular-shaped specimens of PMMA, PMMA/SOY composites, and PMMA/AN -*g*-SOY composites that were subjected to a heating cycle with a rate of 3 °C/min at a frequency of 1 Hz. Comparing the DMA results of the different samples, the storage modulus (E') values were found to be higher for the PMMA/SOY composites and PMMA/AN-*g*-SOY composites. The effect of graft copolymerization of acrylonitrile on the storage modulus of SOY/AN-*g*-SOY composites can be easily observed by comparing the representative data. The enhancement in the storage modulus was attributed to the reinforcing effect of pristine SOY/AN-*g*-SOY in the following order SOY < AN-*g*-SOY. The higher storage modulus in the case of AN-*g*-SOY is attributed to the enhanced compatibility between the pristine PMMA and hydrophobic AN-*g*-SOY reinforcement. The better compatibility between the PMMA matrix and AN-*g*-SOY facilitates the load transfer at the interphase resulting in an increase in the stiffness of the resulting composites material.[34] In the case of the pristine SOY-reinforced composites, the poor dispersion of SOY and poor interfacial interaction between the SOY and PMMA matrix lead to the lesser storage modulus. The damping coefficient of both the PMMA/SOY composites and PMMA/AN -*g*-SOY composites was also found to be similar to the pristine PMMA. The damping coefficient (tan $\delta = E''/E$) in the SOY/AN-*g*-SOY composite was found to reach an optimum value as the storage modulus (E') decreases due to the fact that at higher temperature the molecular segments are quite free to move.[35] Furthermore, the well-interfacial adhesion between AN-*g*-SOY and the PMMA matrix may limit the movement of polymer molecular chains resulting in increased molecular segmental friction.

CONCLUSION

Soy flour is an abundant, environmental friendly, economic, and biorenewable material. Different kinds of soy-based materials have attracted considerable attention of industry in the fields of packaging, biomedicine, and food. However, little efforts have been put to using soy flour as a reinforcing material due to its hydrophilic nature. In this work, soy flour was modified with an acrylonitrile monomer to overcome its shortcoming for its multifunctional applications in polymer composites. From this study, it was concluded that SOY can be easily grafted with acrylonitrile to incorporate the desired hydrophobic functionalities using APS as the reaction initiator. Different parameters were optimized to get the optimum percentage of grafting (152%), and it was determined that each reaction parameter plays an important role in determining the overall percentage of grafting. AN-*g*-SOY was further used as a reinforcement in a PMMA polymer matrix, and the resulting composites exhibited enhanced dynamic mechanical properties compared to the pristine SOY-reinforced PMMA polymer composites.

AUTHOR INFORMATION

Corresponding Author

*Tel.: +1 509 335 8654. Fax: +1 509 335 4662. E-mail: MichaelR.Kessler@wsu.edu.

Notes

The authors declare no competing financial interest.

ACKNOWLEDGMENTS

This material is based upon work supported by the National Science Foundation under Grant CMMI1348747.

REFERENCES

(1) Zhang, X.; He, Q.; Gu, H.; Colorado, H. A.; Wei, S.; Guo, Z. Flame-retardant electrical conductive nanopolymers based on bisphenol epoxy resin reinforced with nano polyanilines. *ACS Appl. Mater. Interfaces* **2013**, *5*, 898−910.

(2) He, Q.; Yuan, T.; Wei, S.; Guo, Z. Catalytic and synergistic effects on thermal stability and combustion behavior of polypropylene: Influence of maleic anhydride grafted polypropylene stabilized cobalt nanoparticles. *J. Mater. Chem. A* **2013**, *1*, 13064−13075.

(3) Zhu, J.; Wei, S.; Lee, I. Y.; Park, S.; Willis, J.; Haldolaarachchige, N.; Young, D. P.; Luo, Z.; Guo, Z. Silica stabilized iron particles toward anti-corrosion magnetic polyurethane nanocomposites. *RSC Adv.* **2012**, *2*, 1136−1143.

(4) An, Q.; Rider, A. N.; Thostenson, E. T. Hierarchical composite structures prepared by electrophoretic deposition of carbon nanotubes onto glass fibers. *ACS Appl. Mater. Interfaces* **2013**, *5*, 2022−2032.

(5) Thakur, V. K.; Vennerberg, D.; Madbouly, S. A.; Kessler, M. R. Bio-inspired green surface functionalization of PMMA for multifunctional capacitors. *RSC Adv.* **2014**, *4*, 6677−6684.

(6) Lasater, K. L.; Thostenson, E. T. In situ thermoresistive characterization of multifunctional composites of carbon nanotubes. *Polymer* **2012**, *53*, 5367−5374.

(7) Pandey, G.; Thostenson, E. T. Carbon nanotube-based multifunctional polymer nanocomposites. *Polym. Rev.* **2012**, *52*, 355−416.

(8) Thakur, V. K.; Singha, A. S.; Mehta, I. K. Renewable resource-based green polymer composites: Analysis and characterization. *Int. J. Polym. Anal. Charact.* **2010**, *15*, 137−146.

(9) Depan, D.; Shah, J. S.; Misra, R. D. K. Degradation mechanism and increased stability of chitosan-based hybrid scaffolds cross-linked with nanostructured carbon: Process-structure-functional property relationship. *Polym. Degrad. Stab.* **2013**, *98*, 2331−2339.

(10) Misra, R. D. K.; Depan, D.; Shah, J. The effect of dimensionality of nanostructured carbon on the architecture of organic-inorganic hybrid materials. *Phys. Chem. Chem. Phys.* **2013**, *15*, 12988−12997.

(11) Thakur, V. K.; Thakur, M. K.; Gupta, R. K. Rapid synthesis of graft copolymers from natural cellulose fibers. *Carbohydr. Polym.* **2013**, *98*, 820−828.

(12) Cosutchi, A. I.; Hulubei, C.; Stoica, I.; Ioan, S. Morphological and structural-rheological relationship in Epiclon-based polyimide/hydroxypropylcellulose blend systems. *J. Polym. Res.* **2010**, *17*, 541−550.

(13) Dobos, A. M.; Onofrei, M.-D.; Stoica, I.; Olaru, N.; Olaru, L.; Ioan, S. Rheological properties and microstructures of cellulose acetate phthalate/hydroxypropyl cellulose blends. *Polym. Compos.* **2012**, *33*, 2072−2083.

(14) Kumar, A. P.; Depan, D.; Singh, R. P. Durability of natural fiber-reinforced composites of ethylene-propylene copolymer under accelerated weathering and composting conditions. *J. Thermoplast. Compos. Mater.* **2005**, *18*, 489−508.

(15) Zhang, X.; Bitaraf, V.; Wei, S.; Guo, Z.; Zhang, X.; Wei, S.; Colorado, H. A. Vinyl ester resin: Rheological behaviors, curing kinetics, thermomechanical, and tensile properties. *AIChE J.* **2014**, *60*, 266−274.

(16) Dobos, A. M.; Stoica, I.; Olaru, N.; Olaru, L.; Ioanid, E. G.; Ioan, S. Surface properties and biocompatibility of cellulose acetates. *J. Appl. Polym. Sci.* **2012**, *125*, 2521−2528.

(17) Depan, D.; Kumar, B.; Singh, R. P. Preparation and characterization of novel hybrid of chitosan-g-PDMS and sodium montmorrilonite. *J. Biomed. Mater. Res., Part B* **2008**, *84B*, 184−190.

(18) Zhang, X.; Alloul, O.; He, Q.; Zhu, J.; Verde, M. J.; Li, Y.; Wei, S.; Guo, Z. Strengthened magnetic epoxy nanocomposites with protruding nanoparticles on the graphene nanosheets. *Polymer* **2013**, *54*, 3594−3604.

(19) Bajpai, P. K.; Singh, I. Drilling behavior of sisal fiber-reinforced polypropylene composite laminates. *J. Reinf. Plast. Compos.* **2013**, *32*, 1569−1576.

(20) Thakur, V. K.; Thakur, M. K.; Gupta, R. K. Graft copolymers of natural fibers for green composites. *Carbohydr. Polym.* **2014**, *104*, 87−93.

(21) Thakur, V. K.; Singha, A. S.; Thakur, M. K. Fabrication and physico-chemical properties of high-performance pine needles/green polymer composites. *Int. J. Polym. Mater.* **2013**, *62*, 226−230.

(22) Nesterenko, A.; Alric, I.; Silvestre, F.; Durrieu, V. Comparative study of encapsulation of vitamins with native and modified soy protein. *Food Hydrocoll.* **2014**, *38*, 172−179.

(23) Kim, J. T.; Netravali, A. N. Development of aligned-hemp yarn-reinforced green composites with soy protein resin: Effect of pH on mechanical and interfacial properties. *Compos. Sci. Technol.* **2011**, *71*, 541−547.

(24) Thakur, V. K.; Grewell, D.; Thunga, M.; Kessler, M. R. Novel Composites from eco-friendly soy flour/SBS triblock copolymer. *Macromol. Mater. Eng.* **2014**, *299*, 953−958.

(25) Thakur, V. K.; Thunga, M.; Madbouly, S. A.; Kessler, M. R. PMMA-g-SOY as a sustainable novel dielectric material. *RSC Adv.* **2014**, *4*, 18240−18249.

(26) Dastidar, T. G.; Netravali, A. N. A soy flour based thermoset resin without the use of any external crosslinker. *Green Chem.* **2013**, *15*, 3243−3251.

(27) Kim, J. T.; Netravali, A. N. Effect of protein content in soy protein resins on their interfacial shear strength with ramie fibers. *J. Adhes. Sci. Technol.* **2010**, *24*, 203−215.

(28) Kim, J. T.; Netravali, A. N. Mechanical, thermal, and interfacial properties of green composites with ramie fiber and soy resins. *J. Agric. Food Chem.* **2010**, *58*, 5400−5407.

(29) Thakur, V. K.; Thakur, M. K.; Gupta, R. K. Graft copolymers from cellulose: Synthesis, characterization and evaluation. *Carbohydr. Polym.* **2013**, *97*, 18−25.

(30) Thakur, V. K.; Thakur, M. K.; Gupta, R. K. Synthesis of lignocellulosic polymer with improved chemical resistance through free radical polymerization. *Int. J. Biol. Macromol.* **2013**, *61*, 121−126.

(31) Thakur, V. K.; Thakur, M. K.; Gupta, R. K. Development of functionalized cellulosic biopolymers by graft copolymerization. *Int. J. Biol. Macromol.* **2013**, *62*, 44−51.

(32) Thakur, V. K.; Singha, A. S.; Kaur, I.; Nagarajarao, R. P.; Liping, Y. Silane functionalization of *Saccaharum cilliare* fibers: Thermal, morphological, and physicochemical study. *Int. J. Polym. Anal. Charact.* **2010**, *15*, 397−414.

(33) Thakur, V. K.; Thakur, M. K.; Gupta, R. K. Graft copolymers from natural polymers using free radical polymerization. *Int. J. Polym. Anal. Charact.* **2013**, *18*, 495−503.

(34) Cui, H.; Kessler, M. R. Glass fiber reinforced ROMP-based bio-renewable polymers: Enhancement of the interface with silane coupling agents. *Compos. Sci. Technol.* **2012**, *72*, 1264−1272.

(35) Martínez-Hernández, A. L.; Velasco-Santos, C.; de-Icaza, M.; Castaño, V. M. Dynamical−mechanical and thermal analysis of polymeric composites reinforced with keratin biofibers from chicken feathers. *Composites, Part B* **2007**, *38*, 405−410.